

Published in final edited form as:

Biochim Biophys Acta. 2010 July ; 1804(7): 1537–1541. doi:10.1016/j.bbapap.2010.03.005.

Restricted domain mobility in the *Candida albicans* Ess1 prolyl isomerase

Lynn McNaughton^a, Zhong Li^a, Patrick Van Roey^a, Steven D. Hanes^{a,b}, and David M. LeMaster^{a,b}*

^aWadsworth Center, New York State Department of Health, University at Albany, Empire State Plaza, Albany, New York, 12201. USA

^bDepartment of Biomedical Sciences, School of Public Health, University at Albany, Empire State Plaza, Albany, New York, 12201. USA

Abstract

Ess1 is a peptidyl prolyl *cis/trans* isomerase that is required for virulence of the pathogenic fungi *Candida albicans* and *Cryptococcus neoformans*. The enzyme isomerizes the phospho-Ser-Pro linkages in the C-terminal domain of RNA polymerase II. Its human homolog, Pin1, has been implicated in a wide range of human diseases, including cancer and Alzheimer's disease. Crystallographic and NMR studies have demonstrated that the sequence linking the catalytic isomerase domain and the substrate binding WW domain of Pin1 is unstructured and that the two domains are only loosely associated in the absence of the substrate. In contrast, the crystal structure of *C. albicans* Ess1 revealed a highly ordered linker that contains a three turn α -helix and extensive association between the two tightly juxtaposed domains. In part to address the concern that the marked differences in the domain interactions for the human and fungal structures might reflect crystal lattice effects, NMR chemical shift analysis and ¹⁵N relaxation measurements have been employed to confirm that the linker of the fungal protein is highly ordered in solution. With the exception of two loops within the active site of the isomerase domain, the local backbone geometry observed in the crystal structure appears to be well preserved throughout the protein chain. The marked differences in interdomain interactions and linker flexibility between the human and fungal enzymes provide a structural basis for therapeutic targeting of the fungal enzymes.

Keywords

prolyl isomerase; NMR; flexibility; domain; chemical shift; ¹⁵N relaxation

1. Introduction

Ess1 is a peptidyl prolyl *cis/trans* isomerase (PPIase) that is essential for viability in the budding yeast *Saccharomyces cerevisiae* [1,2], where it plays a critical role in regulation of gene

© 2010 Elsevier B.V. All rights reserved.

*To whom correspondence should be addressed. lemaster@wadsworth.org. Telephone: +001-518-474-6396. Fax: +001-518-473-2900.

Publisher's Disclaimer: This is a PDF file of an unedited manuscript that has been accepted for publication. As a service to our customers we are providing this early version of the manuscript. The manuscript will undergo copyediting, typesetting, and review of the resulting proof before it is published in its final citable form. Please note that during the production process errors may be discovered which could affect the content, and all legal disclaimers that apply to the journal pertain.

Appendix A. Supplementary data

Supplementary data associated with this article can be found, in the online version, at

transcription by RNA polymerase II [3]. Ess1 binds to the carboxy terminal domain of the largest subunit of RNA pol II [3–5] and controls protein association via its isomerization activity at the phospho-Ser-Pro peptide bond in the heptad (Tyr-pSer-Pro-Thr-pSer-Pro-Ser) repeat segment [6]. The human homolog of Ess1, called Pin1, binds to a wide range of proteins that have been implicated in human disease states, including cancer and Alzheimer's disease. As a result, Pin1 has become an active focus of therapeutic drug development [7,8].

Ess1 is required for the virulence of the pathogenic fungi *Candida albicans* and *Cryptococcus neoformans*, which cause life-threatening infections in humans [9,10]. Immunocompromised patients are particularly susceptible to these pathogens, and although several potent antifungal drugs are available for clinical use, drug resistance is an escalating problem [11,12]. All clinically used inhibitors target the fungal cell wall and membrane pathways. The development of inhibitors that target other pathways would be useful for combination therapies [13]. If the differences in conformation that have been observed between the human Pin1 and fungal Ess1 enzymes in the crystal state are maintained under more physiological conditions, these structural variations may enable Ess1 to be exploited as a viable alternate target for drug development.

X-ray crystallographic analyses [14,15] of the human Pin1 enzyme reveal a two-domain structure containing a prolyl isomerase catalytic domain and a smaller WW domain that tightly binds peptides containing the phospho-Ser/Thr-Pro motif. The two domains are linked by a conformationally disordered segment of about 12 residues, including four residues for which no electron density could be observed. Although the WW and PPIase domains are closely packed together in the crystal structure, NMR studies [16,17] demonstrate that in the absence of substrate binding there is extensive conformational flexibility in this linker segment, and few stable interactions occur between the two domains. However, when cognate peptides are bound, correlated molecular tumbling of the two domains is induced.

The X-ray structure of the apo- form of the *C. albicans* Ess1 enzyme [18] reveals a linker region that is 11 residues longer than that of Pin1. In marked contrast to the human enzyme, the linker segment of Ess1 is well-ordered in the X-ray structure and includes a three-turn α -helix. Furthermore, the juxtaposition of the WW and PPIase domains differs substantially from the packing observed in the Pin1 crystal structure, resulting in much more extensive interdomain interactions. The clearly defined electron density throughout the linker segment suggests limited flexibility in the relative orientation of the two domains, with the result that the active site of the PPIase domain and the peptide binding site of the WW domain are rigidly separated by ~ 50 Å.

In marked contrast, the flexibility of the linker in Pin1 enables the WW and PPIase domains to reorient largely independently of one another [16,17]. The distance between the active site of the WW domain and that of the PPIase domain in Pin1 varies from 20 Å to 81 Å among ten solution NMR structures (pdb code 1NMV [17]) and the crystal structure (pdb code 1PIN [14]). This suggests that the two Pin1 domains can re-position themselves to optimize the relative orientation and separation of the primary substrate recognition site and the active site so as to obtain enhanced activity. To exploit this structural variability, bivalent ligands have been designed that simultaneously bind to both domains of Pin1 with affinities in the nanomolar range [19]. The resultant affinities depend upon the length of the polyproline linker that tethers the WW- and PPIase-directed ends of the ligand.

If pharmaceutical design is to make use of the suggested difference in interdomain mobility for the human Pin1 and fungal Ess1 enzymes, it is important to demonstrate that the sequence linking the two domains in Ess1 indeed lacks conformational flexibility and that the conformation of the enzyme in solution is consistent with that found in the crystal. Here, we

report NMR analysis of *C. albicans* Ess1 which demonstrates that the conformation and flexibility of the fungal enzyme in solution is consistent with that anticipated from the crystallographic structure.

2. Materials and methods

2.1. Recombinant protein expression and purification

Construction of the Ess1 expression plasmid and protein purification were carried out as previously described [18]. In summary, following growth at 22°C to an optical density of 0.6 at 600 nm, 0.5 mM isopropylthiogalactoside was added and expression of the Ess1 protein proceeded for 4 hours. After cell lysis, the His-tagged fusion protein was initially purified on a Ni²⁺-NTA affinity column. Following thrombin digestion, the Ess1 protein was further purified by gel filtration. For uniform ¹⁵N labeling, strain BL21 (DE3), bearing the pCaEss1 expression plasmid, was grown in M9 minimal medium containing 1.2 g / L of ¹⁵NH₄Cl. The carbon source was changed to 2 g / L of [U-¹³C] glucose for expression of the ¹³C labeled protein sample. The protein samples were equilibrated in 50 mM potassium phosphate buffer pH 6.50 containing 5 mM dithiothreitol-d₁₀ and 7% ²H₂O and then concentrated to 0.5 mM by centrifugal centrifugation for NMR data collection.

2.2. NMR data collection and backbone resonance assignment

NMR resonance assignment and relaxation experiments were recorded at 25°C with a Bruker Avance 600 MHz spectrometer and a Bruker Avance II 800 MHz spectrometer, both equipped with triple resonance cryoprobes. Experimental data were processed with Felix software (Felix NMR, Inc.). The ¹³C and ¹⁵N chemical shifts were referenced indirectly using the γ_{13C}/γ_{1H} and γ_{15N}/γ_{1H} ratios, respectively [20]. 2D ¹H-¹⁵N HSQC, 3D HNC0, HN(CA)CO, HNCACB and HN(CO)CACB experiments were carried out to establish backbone resonance assignments for all nonproline residues, excepting residues Arg 18, Ser 19 and His 20 in loop 1 of the WW domain. The ¹H, ¹³C and ¹⁵N backbone resonance assignments of the *C. albicans* Ess1 prolyl isomerase have been deposited in the BioMagResBank (accession number 16690). 3D HBHA (CO)NH, HC(C)H-TOCSY and (H)CCH-TOCSY experiments were used to establish a partial assignment of the sidechain ¹H and ¹³C resonances as well.

2.3. NMR relaxation measurements and analysis

Backbone amide T₁ and T₂ relaxation measurements [21] were carried out with the use of a recycle delay of 1.6 sec. Longitudinal relaxation delays of 0.05, 0.08, 0.13, 0.20, 0.08, 0.30, 0.50, 0.80, 0.30, and 1.35 sec were used. Delays of 16.96, 33.92, 50.88, 16.96, 84.80, 118.72, 152.64, 84.8, and 186.56 msec were used to measure transverse relaxation. The exponential decay constants were estimated using Monte Carlo analysis of the uncertainties with the Curvefit program [22]. {¹H}-¹⁵N NOE relaxation measurements [21] were collected in duplicate to provide uncertainty estimates, using a 5.0 sec recycle delay.

Order parameter analysis was carried out with the Modelfree program [23]. An axially symmetric molecular diffusion tensor analysis was applied, using coordinates derived from the X-ray structure [18]. Hydrogens were introduced into the structure with the Reduce program [24]. An axial diffusion ratio of 1.31 and an effective molecular correlation time of 11.8 ns were obtained. The optimal dynamical model for analysis of each backbone amide was assigned according to the previously described protocol [23].

3. Results and discussion

3.1. Chemical shift analysis of the Ess1 prolyl isomerase backbone conformation

The chemical shifts of the ^1H , ^{13}C and ^{15}N resonances of a protein are well known to be acutely sensitive to secondary and tertiary structure. The chemical shifts for the ^{13}C and ^{15}N resonances of the backbone atoms have long been used to identify the α -helical and β -sheet segments of the chain [25]. The sensitivity of these chemical shifts to the local backbone conformation is such that reasonably robust predictions of the ϕ and ψ dihedral angles of individual residues can be obtained. On average, only about 2% of the (ϕ, ψ) predictions of the TALOS algorithm [26] differ substantially from the values found in the X-ray structures. When combined with robust *a priori* protein modeling algorithms, chemical shifts can provide efficient experimental filters for identifying accurate tertiary structures [27,28].

To examine the consistency between the Ess1 structure in the solution and crystal states, we assigned the ^1H , ^{13}C and ^{15}N backbone resonances and analyzed the chemical shifts of the resonances with the TALOS algorithm. In panel B of Figure 1 are displayed the ϕ and ψ dihedral angles for each residue in the Ess1 X-ray structure. Immediately recognizable are the α -helical segments, which are characterized by comparatively uniform (ϕ, ψ) dihedral angle values. Among these helical segments is that of residues 43 to 55, corresponding to the linker segment helix. The short $\alpha 4$ helix near residue 130 deviates from this pattern of uniform (ϕ, ψ) dihedral angle values, reflecting the fact that this segment is more accurately characterized as a turn containing a single canonical (i, i+3) hydrogen bonding interaction. The remainder of the residues exhibit (ϕ, ψ) dihedral angles that span the typical range of the Ramachandran plot.

Panels C and D of Figure 1 illustrate the difference between the backbone dihedral angles predicted from TALOS analysis of the backbone chemical shifts and those observed in the X-ray structure. Along most of the protein chain, the differences between the chemical shift-predicted and crystallographically observed (ϕ, ψ) dihedral angles are reasonably small. In particular, for residues 43 to 55, the TALOS chemical shift analysis accurately predicts the local backbone geometry of the linker segment helix. With the exception of two loop segments within the PPIase active site, this chemical shift analysis supports the interpretation that the backbone structure of Ess1 is well preserved between crystal and solution.

There are substantial deviations between the X-ray-determined and chemical shift-predicted backbone dihedral angles for a short segment extending from Asp 126 to the start of the $\alpha 4$ helix at His 130 and for a longer segment extends from Ser 80 to Ser 93 (Fig. 1C and 1D). The homologous segments of the human Pin1 sequence are Asp 112 to Ala 116 and Ser 67 to Thr 79, respectively. The shorter loop contains the Cys 113 residue that had been proposed to act as a nucleophile in the catalysis of prolyl isomerization [14], although subsequent mutational analysis [29] has provided support for a non-covalent mechanism of catalysis as has been posited for other prolyl isomerases [30–32].

The X-ray structure of *C. albicans* Ess1 exhibits a closed conformation for the two loop segments within the PPIase active site. Similarly, in the initial X-ray structure of Pin1, determined with an Ala-Pro dipeptide and a sulfate ion bound to the PPIase active site [14], the catalytic loop spanning residues 64–80 adopted a closed conformation, partially surrounding the pseudo-substrate. In contrast, the subsequent X-ray structure of Pin1 with a phospho-Ser-Pro containing peptide bound to the WW domain [15] showed that same PPIase catalytic loop had switched from a closed form to an extended open form, despite being far distant from the WW domain peptide binding site. On the other hand, NMR structural analysis [17] of Pin1 in the absence of either the Ala-Pro peptide or sulfate ion indicates that the residues 64–80 of the catalytic loop remain in a closed conformation. These various results indicate a significant degree of conformational plasticity within the active site of the PPIase domain of

Pin1. The disparity between the (ϕ, ψ) backbone dihedral angles predicted from the chemical shift analysis and those observed in the high resolution X-ray structure of the *C. albicans* Ess1 for these active site loop segments suggests conformational variability in this enzyme as well.

3.2. ^{15}N relaxation analysis of the Ess1 prolyl isomerase backbone mobility

At typical magnetic field strengths, the $\{^1\text{H}\} - ^{15}\text{N}$ heteronuclear NOE experiment is maximally sensitive to motions that occur on a timescale of a few hundred ps. When heteronuclear NOE measurements were carried out on Pin1 [16], essentially all of the residues within both the WW domain and the PPIase domain had NOE values around 0.8, consistent with limited internal motion of the individual H-N bond vectors in the sub-ns timeframe. In dramatic contrast, the 12 residues of the linker region between the two domains had NOE values around -0.2 , comparable to the values for the residues at the mobile N-terminus. Similar markedly smaller values for the ^{15}N T_1/T_2 ratios were also reported for the Pin 1 linker segment. These data demonstrate that the backbone of the linker region in Pin1 undergoes extensive reorientation with respect to the remainder of the protein during the timeframe of the overall molecular tumbling of the protein (~ 10 ns).

The analogous ^{15}N heteronuclear NOE measurements on the *C. albicans* Ess1 indicate no comparable difference in conformational dynamics for the region of backbone surrounding the α -helix of the linker segment or anywhere else along the peptide backbone, excepting the mobile N-terminus (Fig. 2 and Supporting Information Table S1). In addition, we conducted ^{15}N T_1 and T_2 measurements to obtain a more quantitative estimate of orientational disorder in the ps-ns timeframe for each H-N bond vector along the backbone, as well as to derive insight into conformational dynamics in the ms timeframe via linebroadening effects.

The elongated shape of the *C. albicans* Ess1 protein implies that the effective molecular tumbling rate, as monitored by NMR relaxation measurements, will be sensitive to the orientation of each $^1\text{H} - ^{15}\text{N}$ bond vector with respect to the major axis of rotational diffusion. Coordinates from the *C. albicans* Ess1 X-ray structure were used in the modeling of rotational diffusion with the ModelFree program [23] applied to the experimental ^{15}N relaxation data. An optimal fit to the relaxation data was found for an axial ratio of 1.31 for the rotational diffusion tensor and an effective molecular correlation time of 11.8 ns, consistent with that expected for a monomeric globular protein of 20 kDa molecular weight. The principal axis of the calculated rotational diffusion tensor closely corresponds to that of the inertial tensor as deduced from the protein X-ray coordinates. Order parameters measuring the extent of orientational disorder of the H-N bond vectors were derived using the standard protocol for the assignment of dynamical models to each vector [23], as implemented in the ModelFree program.

Overall, the S^2 order parameters offer no evidence for large amplitude internal motion along the entire backbone of Ess1 (Fig. 3 and Supporting Information Table S2). Modestly reduced order parameters were observed for a subset of the segments connecting secondary structural elements, including the junctions at either end of the $\alpha 1$ helix of the linker segment. The lack of evidence for substantial internal motion in either the ps-ns timeframe or the μs -ms timeframe offers additional support for the interpretation that the overall structure observed in the crystallographic analysis is well preserved in solution. In an asymmetrically tumbling protein, if the orientations of the individual amide H-N bond vectors are incorrectly modeled with respect to the axis of the molecular diffusion tensor, the resultant errors in the relaxation analysis will manifest themselves as an increase in the apparent internal motion [33]. The absence of apparent enhanced internal motion predicted from the *C. albicans* Ess1 relaxation data is generally consistent with the relative orientations of the individual amide H-N bond vectors agreeing with the orientations observed in the X-ray structure.

Loop 1 in the Pin1 WW domain has been shown to directly interact with the phosphate group of the substrate. No ^{15}N relaxation data are reported for residues Arg 18, Ser 19 and His 20 of this loop in the WW domain of *C. albicans* Ess1. Indeed, no amide resonances are observed for these three residues in the standard 2D ^1H - ^{15}N HSQC spectrum under the experimental conditions used. The absence of amide crosspeaks for these three residues could result from either rapid hydrogen exchange with the bulk solvent, or else from conformational exchange processes occurring in the ms timeframe. Higher sensitivity measurements on the isolated WW domain of Pin1 [34] have demonstrated a strong temperature dependence of the linewidth for the ^1H amide resonances of both the Arg and Ser residues in loop 1, consistent with conformational exchange dynamics in the ms timeframe. Although lowering the temperature for the Ess1 sample below the 25°C value used in this study might serve to enhance these resonances, a corresponding degradation in the quality of the relaxation data for the other resonances of the protein would result.

Although several residues yielded a provisional prediction of a small line broadening effect (R_{ex} of $1\text{--}2\text{ s}^{-1}$) due to conformational dynamics on the ms timescale, none of these residues lies in either of the two loops of the PPIase active site discussed above. In the relaxation dispersion analysis of apo-Pin1, the residues exhibiting the largest linebroadening contribution due to conformational exchange were Gln 75 (R_{ex} of 3.66 s^{-1}) and Glu 76 (R_{ex} of 6.77 s^{-1}) [35]. Relaxation measurements on the substrate-bound Pin1 complex at a higher magnetic field yielded R_{ex} values $> 10\text{ s}^{-1}$ for both of these residues and $> 3\text{ s}^{-1}$ for most of the other residues in the two flexible active site loops (Ser 67 - Thr 79 and Asp 112 - Ala 116).

The present results indicate that the loop consisting of residues 67 to 79 of Pin1 undergoes more extensive motion in the ms timeframe than does the corresponding loop in *C. albicans* Ess1. This apparent decrease in conformational flexibility for the fungal enzyme may be explained, at least in part, by the presence of Pro 89 in the Ess1 sequence, which corresponds to an insertion between Gln 75 and Glu 76 in the Pin1 sequence. The conformationally restrained proline residue in the Ess1 sequence is positioned between the two residues for which the homologous residues in human Pin1 exhibit the largest R_{ex} values observed in the protein. The backbone geometry for these loop segments in the PPIase active site of Ess1 that is predicted from chemical shift analysis deviates significantly from that seen in the X-ray structure. These variations may arise from either crystal lattice-induced differences in the average local structure for these loop segments or from an averaging among multiple conformations that occurs in solution within a timeframe that does not appreciably contribute to NMR relaxation under typical experimental conditions.

4. Concluding remarks

The X-ray crystal structure of *C. albicans* Ess1 [18] revealed an α -helical conformation for residues 43 to 55 for which the corresponding sequence in the human Pin1 enzyme forms the unstructured linker segment [14,15]. Subsequent secondary structure predictions for the same segment of other fungal Ess1 enzymes suggested that the linker segment helix is conserved among the pathogenic fungi [18]. NMR studies on a fragment of the homologous PinA enzyme from *Aspergillus nidulans*, containing the WW domain and an additional ~ 15 residues, reported backbone chemical shifts and inter-residue NOE crosspeaks consistent with an α -helix in the analogous position along the sequence [36]. The chemical shift analysis of the full length *C. albicans* enzyme is consistent with the backbone conformation in the crystal structure being well preserved in solution not only for the interdomain linker segment but throughout nearly all of the protein.

In marked contrast to human Pin 1 [16,17], ^{15}N relaxation analysis of the Ess1 enzyme indicates that the asymmetric tumbling of the protein occurs as a single molecular unit. ^{15}N relaxation

analysis of Ess1 indicates quite restricted internal dynamics on both the ps-ns and ms timescales. The only apparent substantial exception to this restricted mobility occurs for three residues in the substrate-binding loop 1 of the WW domain. As a result, the differences between the yeast and human enzymes in average structure, in conformational dynamics and in the variability for the interdomain interactions may provide a useful basis for the design of selective therapeutic agents for the treatment of pathogenic fungal infections.

Supplementary Material

Refer to Web version on PubMed Central for supplementary material.

Abbreviations

PPIase peptidyl proline isomerase

Acknowledgments

This work was supported in part by the grant GM055108 from the National Institutes of Health (to S. D. H.). We acknowledge the use of the Wadsworth Center NMR facility and the New York Structural Biology Center.

References

- Hanes SD, Shank PR, Bostian KA. Sequence and mutational analysis of ESS1, a gene essential for growth in *Saccharomyces cerevisiae*. *Yeast* 1989;5:55–72. [PubMed: 2648698]
- Hani J, Schelbert B, Bernhardt A, Domdey H, Fischer G, Wiebauer K, Rahfeld JU. Mutations in a peptidylprolyl-cis/trans-isomerase gene lead to a defect in 3'-end formation of a pre-mRNA in *Saccharomyces cerevisiae*. *J. Biol. Chem* 1999;274:108–116. [PubMed: 9867817]
- Wu X, Wilcox CB, Devasahayam G, Hackett RL, Arevalo-Rodriguez M, Cardenas ME, Heitman J, Hanes SD. The Ess1 prolyl isomerase is linked to chromatin remodeling complexes and the general transcription machinery. *EMBO J* 2000;19:3727–3738. [PubMed: 10899126]
- Morris DP, Phatnani HP, Greenleaf AL. Phospho-carboxyl-terminal domain binding and the role of a prolyl isomerase in pre-mRNA 3'-end formation. *J. Biol. Chem* 1999;274:31583–31587. [PubMed: 10531363]
- Gemmill TR, Wu X, Hanes SD. Vanishingly low levels of Ess1 prolyl-isomerase activity are sufficient for growth in *Saccharomyces cerevisiae*. *J. Biol. Chem* 2005;280:15510–15517. [PubMed: 15728580]
- Singh N, Ma Z, Gemmill T, Wu X, DeFiglio H, Rossetini A, Rabeler C, Beane O, Palumbo MJ, Morse RH, Hanes SD. The Ess1 prolyl isomerase is required for transcription termination of small non-coding regulatory RNAs via the Nrd1 pathway. *Mol. Cell* 2009;29:200–209.
- Lu KP. Pinning down cell signaling, cancer and Alzheimer's disease. *Trends Biochem. Sci* 2004;29:200–209. [PubMed: 15082314]
- Wu B, Rega MF, Wei J, Yuan H, Dahl R, Zhang Z, Pellicchia M. Discovery and binding studies on a series of novel Pin1 ligands. *Chem. Biol. Drug Des* 2009;73:369–379. [PubMed: 19291099]
- Devasahayam G, Chaturvedi V, Hanes SD. The Ess1 prolyl isomerase is required for growth and morphogenetic switching in *Candida albicans*. *Genetics* 2002;160:37–48. [PubMed: 11805043]
- Ren P, Chaturvedi V, Hanes SD. The Ess1 prolyl isomerase is dispensible for growth but required for virulence in *Cryptococcus neoformans*. *Microbiol* 2005;151:1593–1605.
- Casalnuovo IA, DiFrancesco P, Garaci E. Fluconazole resistance in *Candida albicans*: A review of mechanisms. *Eur. Rev. Med. Pharmacol* 2004;8:69–77.
- Mathew BP, Nath M. Recent approaches to antifungal therapy for invasive mycoses. *ChemMedChem* 2009;4:310–323. [PubMed: 19170067]
- Kontoyiannis DP, Lewis RE. Toward more effective antifungal therapy: The prospects of combination therapy. *Br. J. Haematol* 2004;126:165–175. [PubMed: 15238137]

14. Ranganathan R, Lu KP, Hunter T, Noel JP. Structural and functional analysis of the mitotic rotamase Pin1 suggests substrate recognition is phosphorylation dependent. *Cell* 1997;89:875–886. [PubMed: 9200606]
15. Verdecia MA, Bowman ME, Lu KP, Hunter T, Noel JP. Structural basis for phosphoserine-proline recognition by group IV WW domains. *Nat. Struct. Biol* 2000;7:639–643. [PubMed: 10932246]
16. Jacobs DM, Saxena K, Vogherr M, Bernado P, Pons M, Fiebig KM. Peptide binding induces large scale changes in inter-domain mobility in human Pin1. *J. Biol. Chem* 2003;278:26174–26182. [PubMed: 12686540]
17. Bayer E, Goettsch S, Mueller JW, Griewel B, Guiberman E, Mayr LM, Bayer P. Structural analysis of the mitotic regulator hPin1 in solution: Insights into domain architecture and substrate binding. *J. Biol. Chem* 2003;278:26183–26193. [PubMed: 12721297]
18. Li Z, Li H, Devasahayam G, Gemmill T, Chaturvedi V, Hanes SD, VanRoey P. The structure of the *Candida albicans* Ess1 prolyl isomerase reveals a well-ordered linker that restricts domain mobility. *Biochemistry* 2005;44:6180–6189. [PubMed: 15835905]
19. Daum S, Lücke C, Wildemann D, Schiene-Fischer C. On the benefit of bivalency in peptide Ligand/Pin1 interactions. *J. Mol. Biol* 2007;374:147–161. [PubMed: 17931657]
20. Wishart DS, Bigam CG, Yao J, Abildgaard F, Dyson HJ, Oldfield E, Markley JL, Sykes BD. H-1, C-13, and N-15 chemical shift referencing in biomolecular NMR. *J. Biomol. NMR* 1995;6:135–140. [PubMed: 8589602]
21. Farrow NA, Muhandiram R, Singer AU, Pascal SM, Kay CM, Gish G, Shoelson SE, Pawson T, Forman-Kay JD, Kay LE. Backbone Dynamics of a Free and a Phosphopeptide-Complexed Src Homology 2 Domain Studied by 15N NMR Relaxation. *Biochemistry* 1994;33:5984–6003. [PubMed: 7514039]
22. Hill RB, Bracken C, DeGrado WF, Palmer IAG. Molecular motions and protein folding: Characterization of the backbone dynamics and folding equilibrium of a₂D using ¹³C NMR spin relaxation. *J. Am. Chem. Soc* 2000;122:11610–11619.
23. Mandel AM, Akke M, Palmer IAG. Backbone dynamics of *Escherichia coli* ribonuclease HI: Correlations with structure and function in an active enzyme. *J. Mol. Biol* 1995;246:144–163. [PubMed: 7531772]
24. Word JM, Lovell SC, Richardson JS, Richardson DC. Asparagine and glutamine: Using hydrogen atom contacts in the choice of side-chain amide orientation. *J. Mol. Biol* 1999;285:1733–1747.
25. Wishart DS, Sykes BD. The 13C Chemical-Shift Index: A simple method for the identification of protein secondary structure using 13C chemical-shift data. *J. Biomolec. NMR* 1994;4:171–180.
26. Cornilescu G, Delaglio F, Bax A. Protein backbone angle restraints from searching a database for chemical shift and sequence homology. *J. Biomolec. NMR* 1999;13:289–302.
27. Cavalli A, Salvatella X, Dobson CM, Vendruscolo M. Protein structure determination from NMR chemical shifts. *Proc. Natl. Acad. Sci U. S. A* 2007;104:9615–9620. [PubMed: 17535901]
28. Shen Y, Lange O, Delaglio F, Rossi P, Aramini JM, Liu GH, Eletsky A, Wu YB, Singarapu KK, Lemak A, Ignatchenko A, Arrowsmith CH, Szyperski T, Montelione GT, Baker D, Bax A. Consistent blind protein structure generation from NMR chemical shift data. *Proc. Natl. Acad. Sci U. S. A* 2008;105:4685–4690. [PubMed: 18326625]
29. Behrsin CD, Bailey ML, Bateman KS, Hamilton KS, Wahl LM, Brandl CJ, Shilton BH, Litchfield DW. Functionally important residues in the peptidyl-prolyl isomerase Pin1 revealed by unigenic evolution. *J. Mol. Biol* 2007;365:1143–1162. [PubMed: 17113106]
30. Stein RL. Mechanism of enzymatic and non-enzymatic prolyl cis-trans isomerization. *Adv. Prot. Chem* 1993;44:1–24.
31. Fischer S, Michnick S, Karplus M. A mechanism for rotamase catalysis by the FK506 binding protein (FKBP). *Biochemistry* 1993;32:13830–13837. [PubMed: 7505615]
32. Schmid FX. Prolyl isomerases. *Adv. Prot. Chem* 2001;59:243–282.
33. Hall JB, Fushman D. Characterization of the overall and local dynamics of a protein with intermediate rotational anisotropy: Differentiating between conformational exchange and anisotropic diffusion in the B3 domain of protein G. *J. Biomol. NMR* 2003;27:261–275. [PubMed: 12975584]
34. Peng T, Zintsmaster JS, Namanja AT, Peng JW. Sequence-specific dynamics modulate recognition specificity in WW domains. *Nat. Struct. Mol. Biol* 2007;14:325–331. [PubMed: 17334375]

35. Labeikovsky W, Eisenmesser EZ, Bosco DA, Kern D. Structure and dynamics of Pin1 during catalysis by NMR. *J. Mol. Biol* 2007;367:1370–1381. [PubMed: 17316687]
36. Ng CA, Kato Y, Tanokura M, Brownlee RTC. Structural characterisation of PinA WW domain and a comparison with other Group IV WW domains. Pin1 and Ess1, *Biochim. Biophys. Acta* 2008;1784:1208–1214.

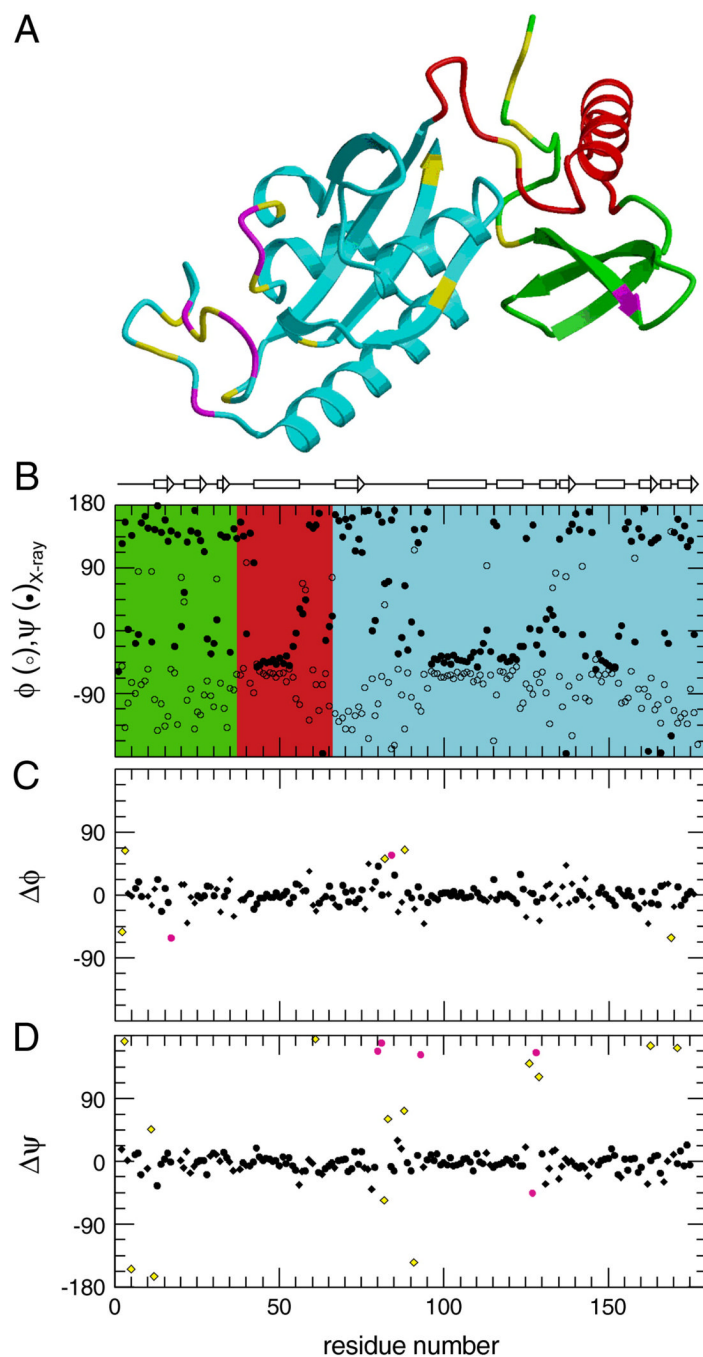


Fig. 1. Chemical shift analysis of backbone geometry for the *C. albicans* Ess1 enzyme. Panel A illustrates the X-ray structure of Ess1 [18] in which residues in the WW domain, linker segment and PPIase domain are indicated in green, red and cyan, respectively. Residues for which TALOS chemical shift analysis [26] strongly predicts differing backbone geometry are indicated in magenta, while tentative discrepancies are marked in yellow. In panel B are shown the backbone dihedral angles ϕ (○) and ψ (●) from the X-ray structure. The sequence positions of the α -helices (cylinders) and β -strands (arrows) are displayed along the top of this panel. In panels C and D are illustrated the differences for the ϕ and ψ dihedral angles in the X-ray structure as compared to those predicted from the chemical shifts. TALOS predictions scored

as good are marked as circles, while tentative predictions are indicated as diamonds. Deviations above 45° are colored magenta or yellow. As is most notable for glycol residues, the TALOS chemical shift analysis is not highly robust in distinguishing between the local mirror images of (ϕ, ψ) and $(-\phi, -\psi)$. In such cases, the mirror conformation that is closest to the X-ray values is displayed.

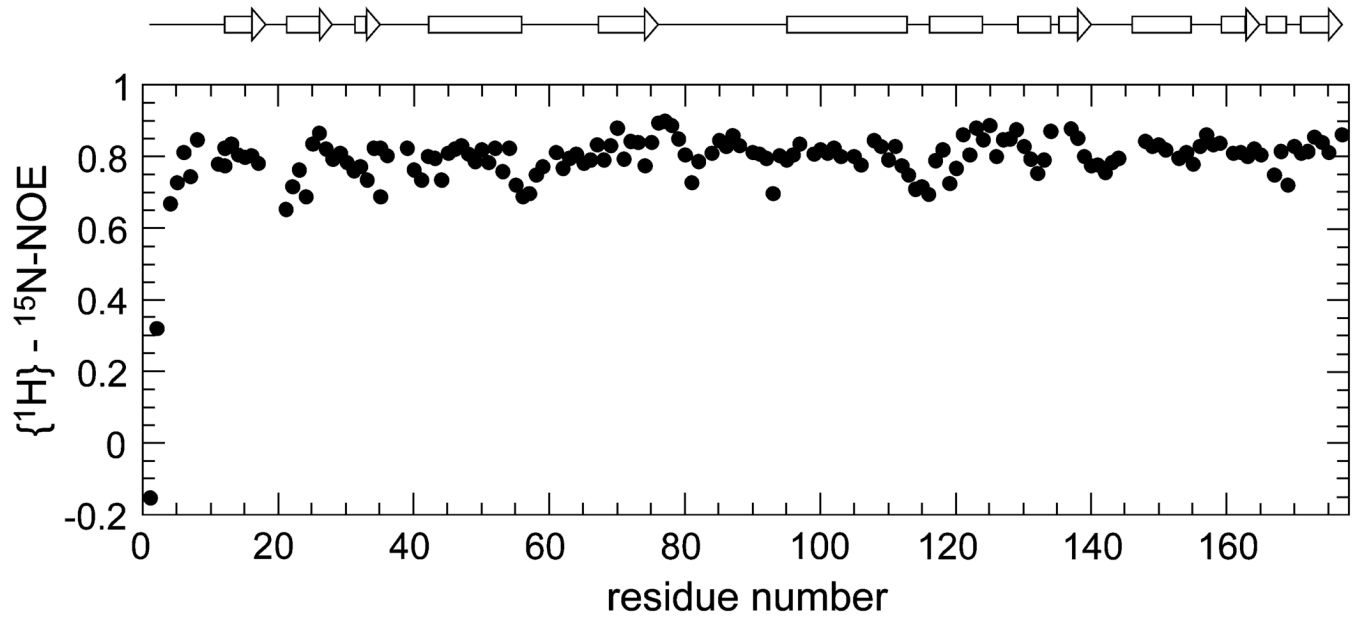


Fig. 2. $\{^1\text{H}\}$ - ^{15}N heteronuclear NOE analysis of the *C. albicans* Ess1 enzyme. With the exception of residues at the N-terminus, the protein backbone indicates only modest internal motion in the timeframe of several hundred ps. The sequence positions of the α -helices (cylinders) and β -strands (arrows) are displayed along the top.

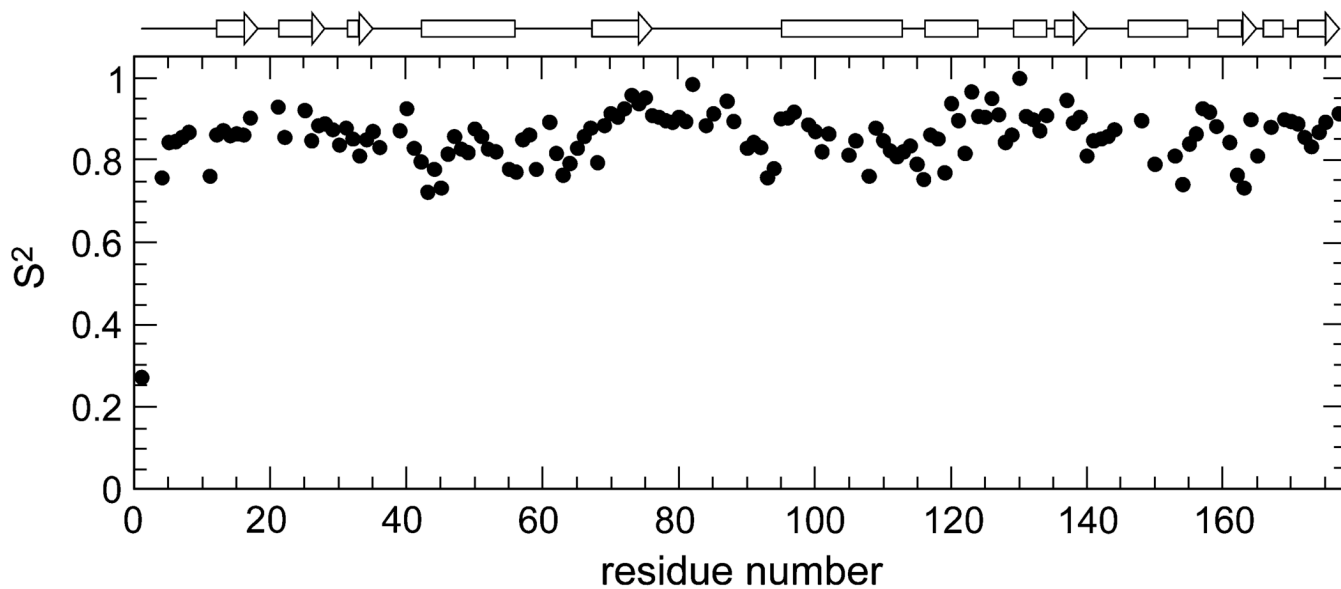


Fig. 3. The ^{15}N relaxation order parameter S^2 values for the *C. albicans* Ess1 enzyme. For each residue, the ^{15}N T_1 , T_2 and heteronuclear NOE data were analyzed in terms of the orientational order parameter S^2 with the ModelFree algorithm using the standard protocol for assignment of dynamical models to each H-N bond vector [23]. The sequence positions of the α -helices (cylinders) and β -strands (arrows) are displayed along the top.